Supplementary Information

Transcription upregulation via force-induced direct stretching of chromatin

Arash Tajik[1, 2#], Yuejin Zhang[1#], Fuxiang Wei[1#], Jian Sun[2#], Qiong Jia[1], Wenwen Zhou[1], Rishi Singh[2], Nimish Khanna[3], Andrew S. Belmont[3*], and Ning Wang[1, 2*]

[1]Department of Biomedical Engineering, School of Life Science and Technology, Huazhong University of Science and Technology, Wuhan, Hubei 430074 China; [2]Department of Mechanical Science and Engineering, University of Illinois at Urbana-Champaign, Urbana, IL 61801 USA; [3]Department of Cell and Developmental Biology, University of Illinois at Urbana-Champaign, Urbana, IL 61801 USA

[#]These authors contributed equally to this work.

[*]Send correspondence to:

Dr. Ning Wang at nwangrw@illinois.edu; or Dr. Andrew Belmont at asbel@illinois.edu

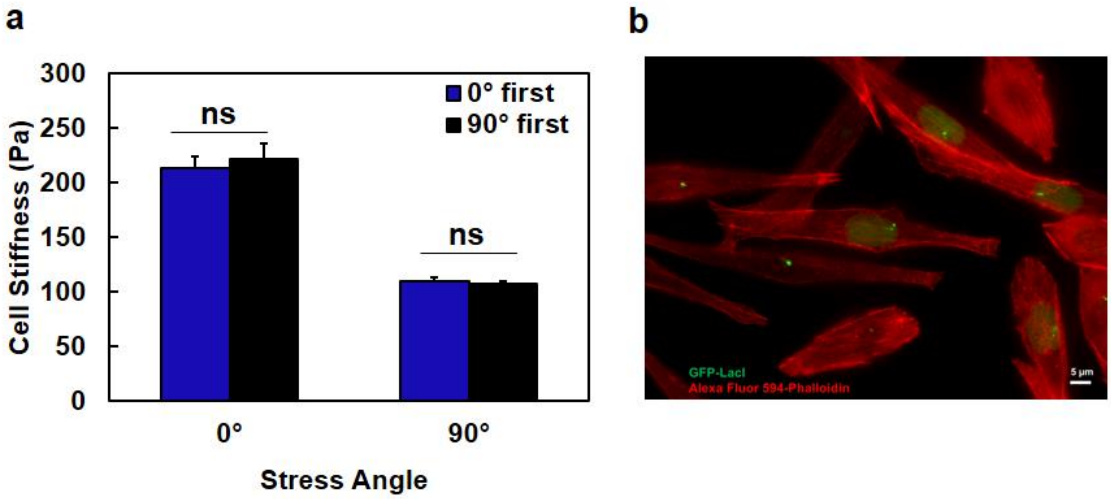

Supplementary Figure 1. CHO cells do not stiffen with stress duration and exhibit stress fibers. (**a**) CHO cells do not stiffen with stress duration (less than 10 min). The sinusoidal oscillatory stress was applied at 15 Pa at 0.3 Hz. The stress was applied in one of two modes: either 0^o first, 90^o second or 90^o first, 0^o second. There were no differences in stiffness values when comparing two modes of stress application. Mean $\pm$ s.e.m; n=13 cells; ns=not statistically significant. (**b**) CHO cells are elongated and exhibit stress fibers along the long axis of the cells. CHO cells were fixed and stained with Alexa Fluor954-Palloidin. The green dots in each cell nucleus were GFP spots in the same chromatin.

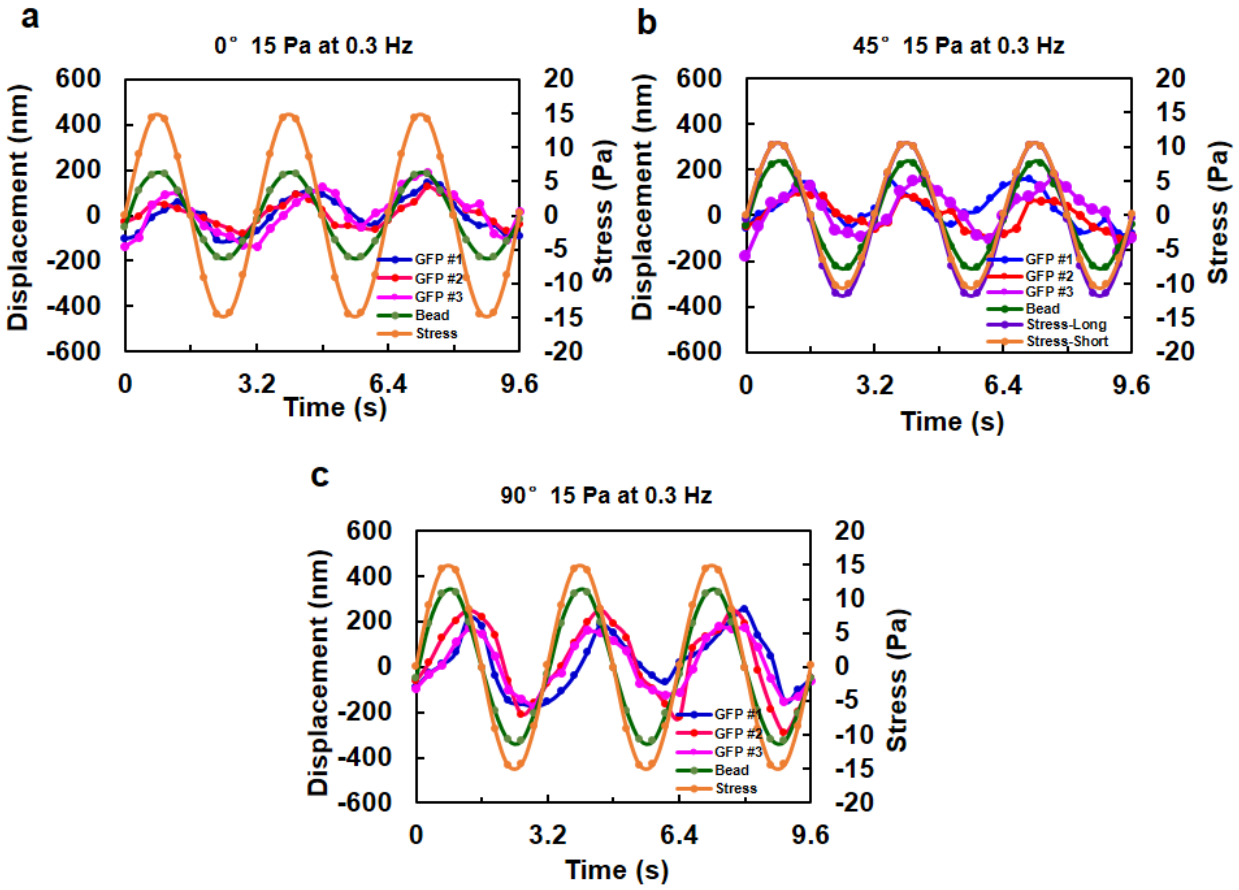

Supplementary Figure 2. Chromatin GFP spots displacements depend on stress angles. A sinusoidal local stress (15 Pa at 0.3 Hz) was applied to the cell surface via a RGD-coated magnetic bead using 3D-MTC and individual chromatin GFP spot displacement was measured by tracking force-induced cyclic movements of the GFP-LacI transgene insertions. Original data of applied stress (orange), bead center displacement (green), displacements of GFP spot #1 (blue), GFP spot #2 (red), GFP spot #3 (pink) were shown in each subfigure. This cell is the same cell as in Fig. 1e. Stress was applied at 0^{o} (**a**), 45^{o} (**b**), or 90^{o} (**c**) relative to the long axis of the cell. A minus-signed stress only represents the fact that it was applied in opposite direction from a plus-signed stress. In (**b**), both X and Y magnetic twisting fields were turned on and both applied a peak stress of 10.6 Pa such that the resultant stress is 15 Pa, same as in (**a**) or (**c**). Note that small (non-sinusoidal) variations in GFP spot displacement curves are possibly due to spontaneous movements of the chromatin.

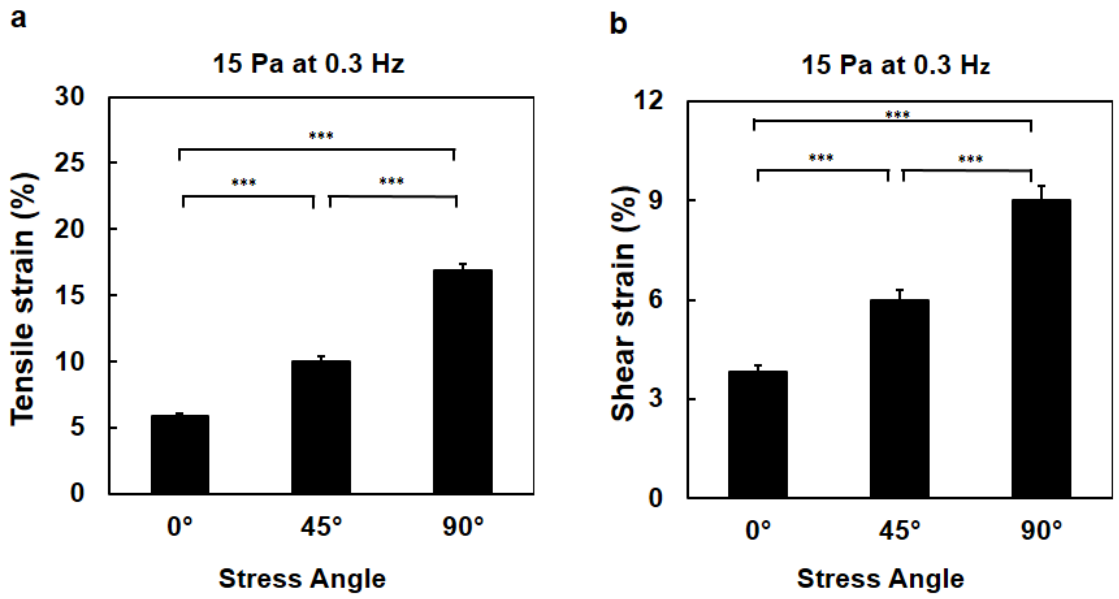

Supplementary Figure 3. Tensile strains dominate chromatin deformation and are stress-angle dependent. (**a**) Tensile strains of the chromatin were computed from stress-induced displacement maps using a published method[13]. Compressive strains were similar in magnitudes. (**b**) Shear strains were computed from the same displacement maps and were ~2.5 times less than tensile strains. Rigid rotation of the chromatin is a measure of rigid body like motions of the chromatin and was lower than shear strains and was not plotted. Mean $\pm$ s.e.m.; n=30 cells; 21 separate experiments. *** $P<0.001$.

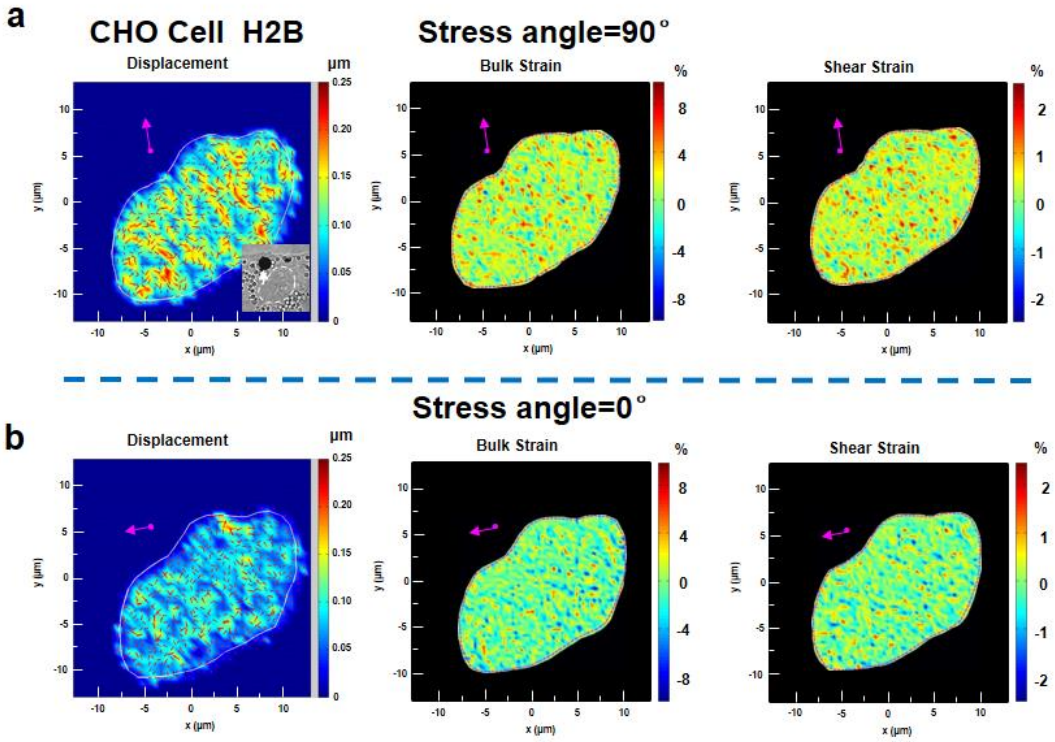

Supplementary Figure 4. Stress-angle dependence of CHO cell H2B deformation. (**a**) A displacement map and strain maps of the CHO cell H2B-GFP when a cyclic stress was applied (15 Pa at 0.1 Hz) at 90^o from the long axis of the cell. Because of large sizes of images, the applied stress could only be applied at 0.1 Hz (and not at 0.3 Hz) in order to capture enough fluorescence intensity. A 4.0-μm RGD-coated magnetic bead was bound to the apical surface of a CHO cell. Inset shows a brightfield image of a portion of the cell; a white arrow points to the bead (black dot); white dashed-lines show the nuclear boundary; a pink arrow points to the direction of the bead center displacement. **Left**: the displacement map; **middle**: the computed 2D bulk strain (2D tensile or compressive strain) map. Note that blue colors or a minus sign of strains indicate that strains are compressive; i.e., the H2Bs are moving closer to each other; **right**: the computed shear strain map. Note that peak shear strains are ~4-fold smaller than bulk strains. (**b**) A displacement map and strain maps of the *same* cell when the same stress was applied at 0^o (along the long axis of the cell). Note that both bulk strains and shear strains are considerable lower than those at 90^o in (**a**). In the absence of applied stress, strains from spontaneous movements were <10% of those strains in the presence of stress: peak bulk strain was <0.08% and peak shear strain was <0.02%. The maximum rigid body rotation of H2B in the presence of stress was <10% of those peak shear strains and was not shown.

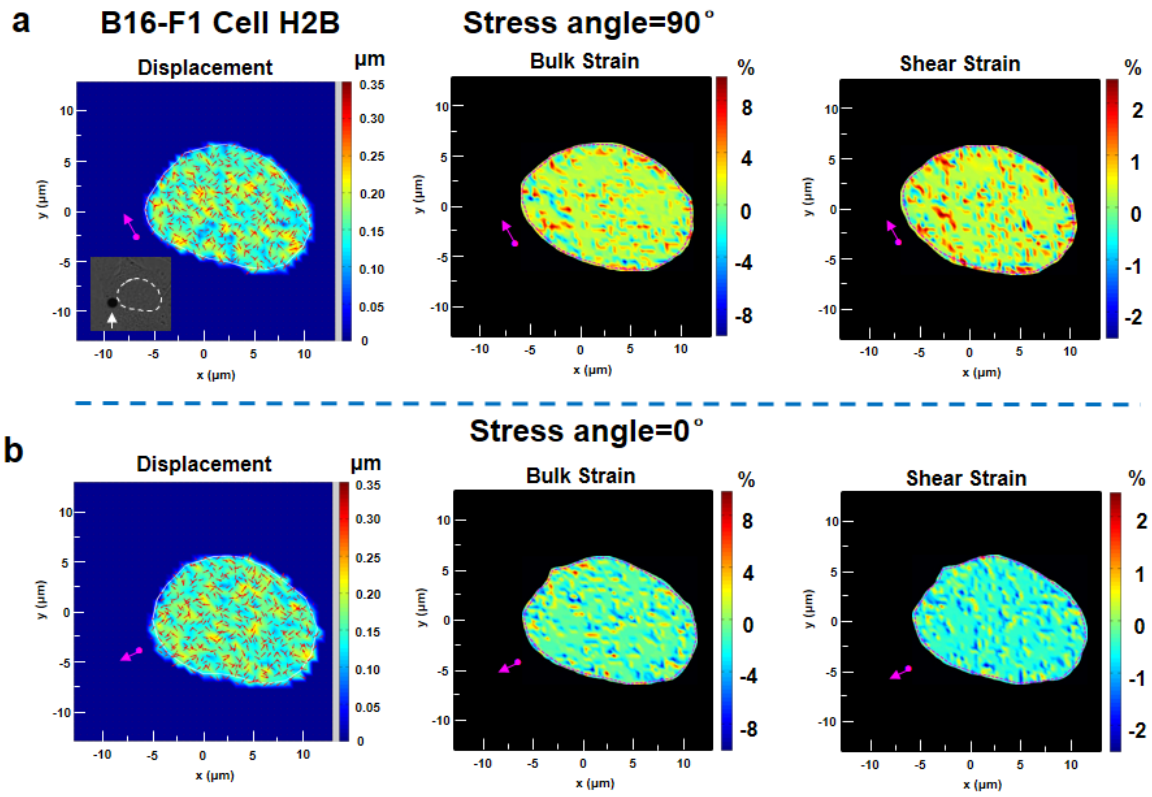

Supplementary Figure 5. Stress-angle dependence of B16 cell H2B deformation. All conditions are the same (15 Pa at 0.1 Hz) as those in Supplementary Fig. 4 except that a B16 cell H2B-GFP was stressed at different angles. (**a**) 90^{o} stress angle. Inset shows the brightfield image of part of the cell. A white arrow points to the bead (black dot); white dashed-lines show the nuclear boundary; a pink arrow points to the direction of the bead center displacement. Dashed lines outline the nuclear boundaries. **Left**: the displacement map; **middle**: the computed bulk strain (2D tensile or compressive strain) map; **right**: the computed shear strains. Note that peak shear strains are ~4-fold smaller than bulk strains. (**b**) A displacement map and strain maps of the *same cell* when the same stress was applied at 0^{o} (along the long axis of the cell). Note that both bulk strains and shear strains are considerable lower than those at 90^{o} in (**a**). In the absence of applied stress, strains from spontaneous movements were <10% of those in the presence of stress: peak bulk strain was <0.08% and peak shear strain was <0.02%. The similarities between Supplementary Figs. 4 and 5 suggest that it is a general feature that bulk strains dominate chromatin deformation in response to the magnetic bead twisting at different angles.

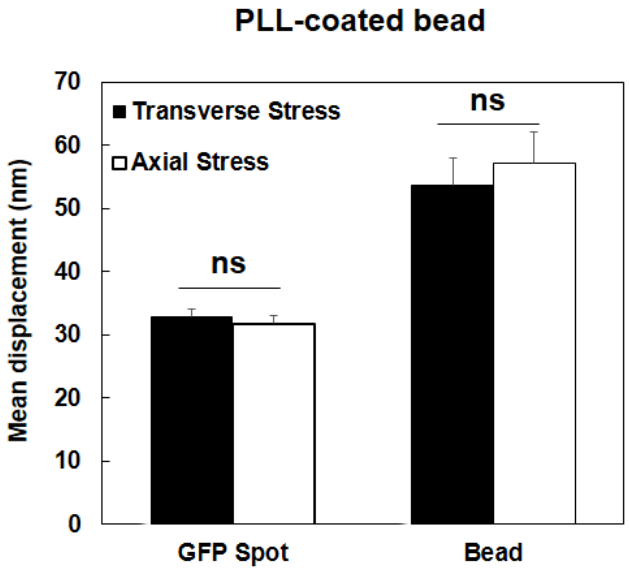

Supplementary Figure 6. Applying a local force nonspecifically does not probe mechanical anisotropy of the cell. A 4.0-μm magnetic bead coated with poly-L-Lysine (PLL) was attached to the apical surface of the cell and a 17.5-Pa stress was applied at 0.3 Hz. A stress angle of 90^{o} (Transverse stress) induced similar bead displacements and GFP spots displacements as a stress angle of 0^{o} (Axial stress, along the long axis of the cell). Mean $\pm$ s.e.m.; n=40 cells and 82 GFP spots for each condition; 3 separate experiments ns=not statistically significant.

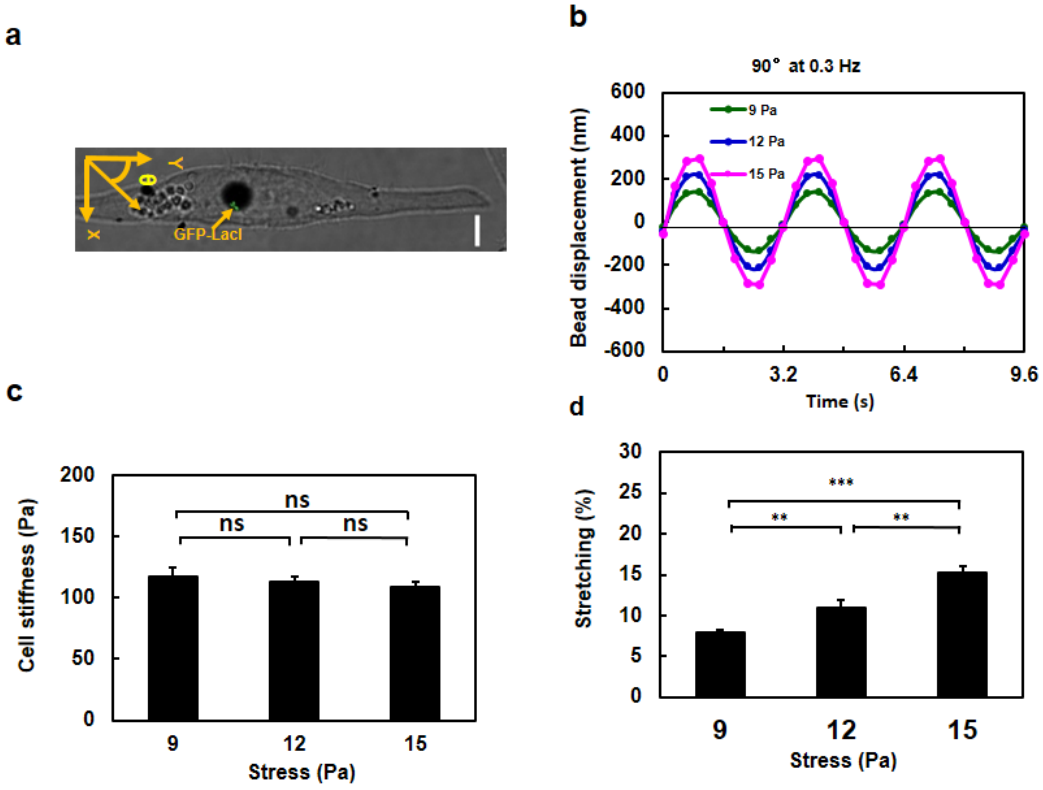

Supplementary Figure 7. Chromatin stretching is stress-amplitude dependent. (**a**) A brightfield image of a representative CHO cell that was stressed by a 4-μm RGD-coated magnetic bead. The bead was magnetized in Z and twisted in X direction so that the stress angle was kept at 90^{o} relative to the cell long axis. Loading frequency was kept at 0.3 Hz. Yellow arrow points to GFP spots. Scale bar, 5 μm. (**b**) Displacements of the bead when applied stress was varied from 9 to 12 to 15 Pa. Varying the sequence of stress amplitudes (e.g., from 12 to 15 to 9 Pa) did not change cell stiffness values. (**c**) Summarized data of the computed cell stiffness. Mean ± s.e.m; n=13 cells; 7 separate experiments; ns=not statistically significant. (**d**) Summarized data of the computed chromatin stretching. Mean ± s.e.m; n=39 GFP spots from 13 cells; 7 separate experiments; ** P<0.01; *** P<0.001.

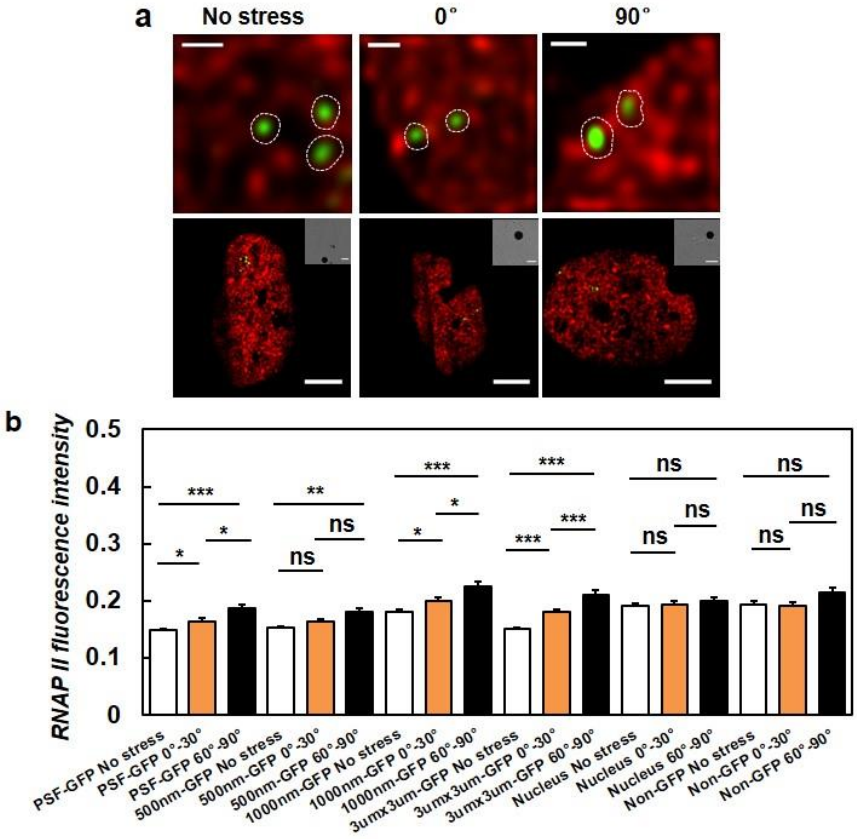

Supplementary Figure 8. RNA Polymerase II binding to GFP spots increases with the extent of chromatin stretching before DHFR transcription upregulation. The stress was applied at 15 Pa at 0.3 Hz for 5 sec. RNA polymerase binding was detected after fixing the cells and staining the cells with anti-RNA polymerase II CTD repeat YSPTSPS (phosphor S5) antibody. (**a**) **Top**, representative fluorescence images of CHO cell GFP LacI (green) and RNA Poly II (red) around the GFP spots. **Left:** no stress; **Middle**: stress applied at 0^o relative to the cell long axis; **Right**: stress applied at 90^o. Scale bars, 500 nm. Dashed lines cover areas within 1.5 x one-half width of the point spread function (**PSF**) of the GFP spots. **Bottom**, representative images of the whole nucleus under various conditions. Scale bars, 5 μm. Insets, brightfield images of the cells, the black dot in each image is a magnetic bead. Scale bar, 5 μm. (**b**) Summarized data of RNA Poly II fluorescence as a function of stress angles. **PSF-GFP**: areas within 1.5 x one half-width PSF of GFP spots. **500nm-GFP**: 500 nm radius away from the center of the GFP spot. **1000nm-GFP**: 1000 nm radius away from the center of the GFP spot. **3μmx3μm-GFP**: a 3 μm x 3 μm area including the GFP spot. **Nucleus**: areas of the whole nucleus at the same focal plane as the GFP spots. **Non-GFP**: 4 randomly chosen areas (3 μm x 3 μm) in each cell >2 μm away from GFP spots. Each cell was stressed only once at one particular angle. **No stress**: the cells bound with RGD coated magnetic beads without applied stresses. Zero fluorescence intensity represents no fluorescence with the background auto-fluorescence subtracted. 1.0 fluorescence intensity represents maximum whiteout intensity. Mean + s.e.m.; n=30 cells per condition for all conditions except for **Non-GFP**; n=10 cells for **Non-GFP**; 3 independent experiments; * P<0.05; ** P<0.01; *** P<0.001; ns= not statistically significant. Note that the peak of RNA poly II binding under stress peaked at 1000 nm from the GFP spots and was not at the closest distance from the GFP spots, suggesting that some of the binding was at the promoter sites of other endogenous genes.

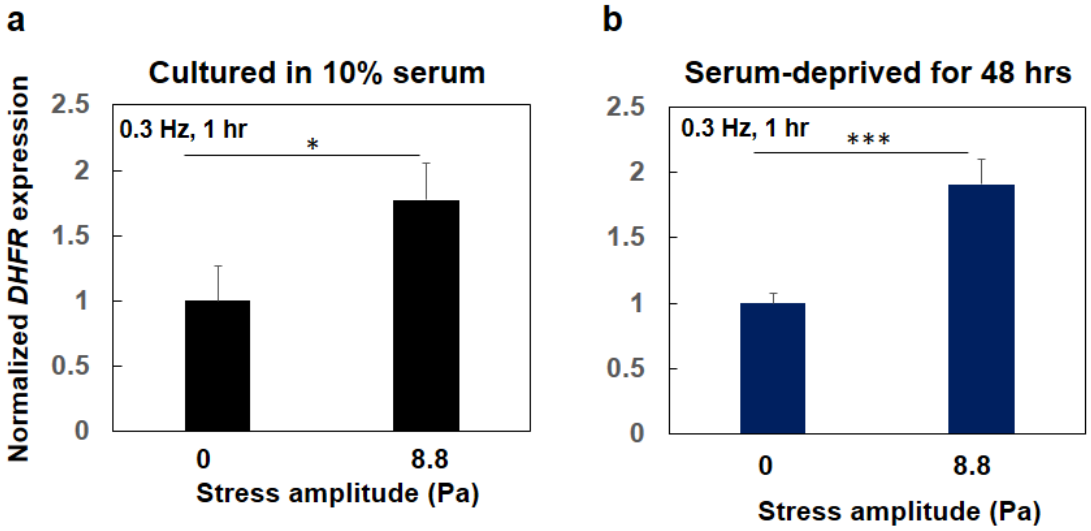

Supplementary Figure 9. Force-induced DHFR transcription elevation does not depend on soluble serum factors. (**a**) CHO cells were cultured in 10% serum before an 8.8-Pa stress was applied at 0.3 Hz for 1 hr. the control cells (**0 stress**) are the cells in the same dish but not bound to any magnetic bead. Mean ± s.e.m.; n=33 (0 stress), 30 (8.8-Pa stress); * $P<0.05$. Note that this subfigure is a re-plot of a part of Fig. 3d for the sole purpose as a reference to the serum-deprivation condition. (**b**) CHO cells were cultured in 0.2% serum for 48 hrs before an 8.8-Pa stress was applied at 0.3 Hz for 1 hr. The control cells (**0 stress**) are the cells in the same dish. The stress induced similar % elevations in DHFR transcription for cells in 0.2% serum and for cells in 10% serum, although baseline DHFR transcription levels in 0.2% serum without stress was ~30% lower than those in 10% serum, consistent with a published report[33]. Mean ± s.e.m.; n=31 (0 stress), 50 (8.8-Pa stress); 3 separate experiments; *** $P<0.001$.

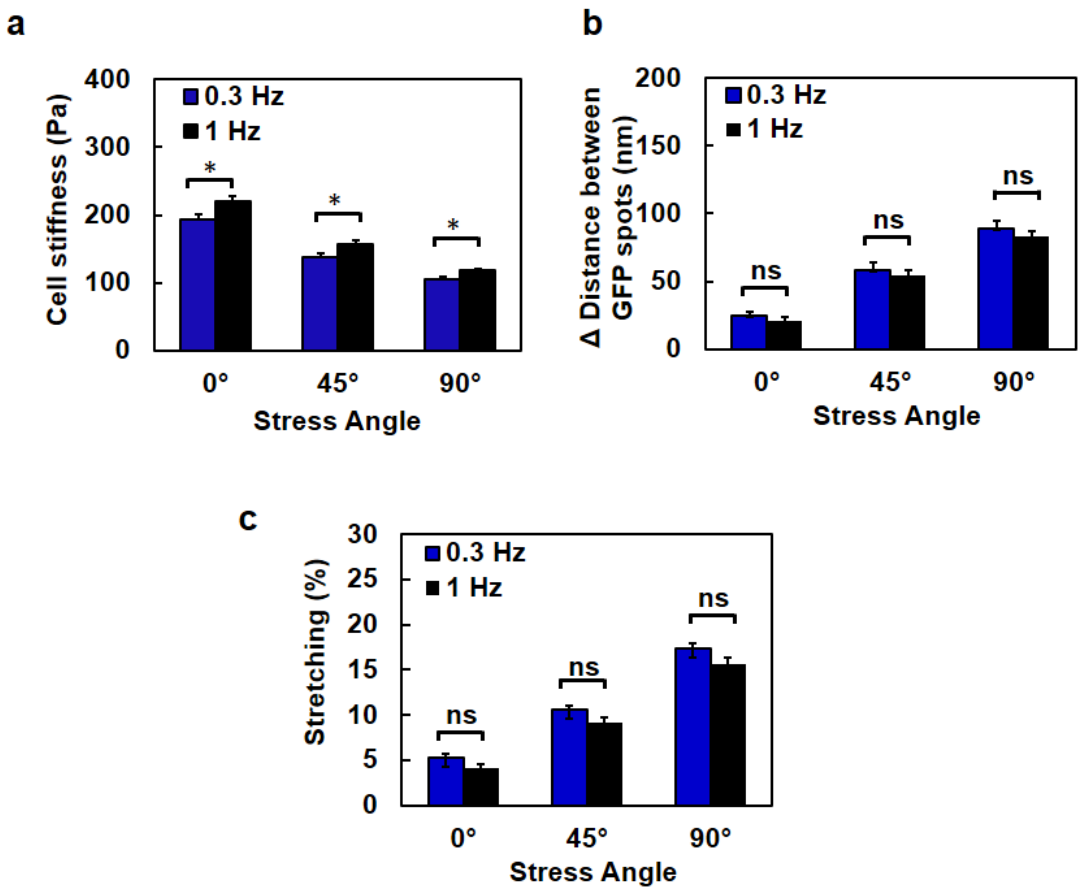

Supplementary Figure 10. Increasing loading frequency does not alter chromatin deformation. (**a**) A local stress was applied to a CHO cell at 15 Pa via RGD-bead-integrin interactions. Cell stiffness was highest at 0^{o} and lowest at 90^{o}, indicating mechanical anisotropy behavior of the cells. Elevating loading frequency increased cell stiffness, suggesting viscoelastic behavior of the cells. Mean $\pm$ s.e.m.; n=10 cells (0.3 Hz); n=10 cells (1 Hz); 8 independent experiments; * P<0.05. (**b** and **c**) No differences are observed in Δ distance between chromatin GFP spots and in % stretching when comparing 0.3 Hz with 1.0 Hz, although both exhibit stress angle dependence. Mean $\pm$ s.e.m.; n=10 cells (0.3 Hz); n=10 cells (1 Hz); 8 independent experiments; ns=not statistically significant.

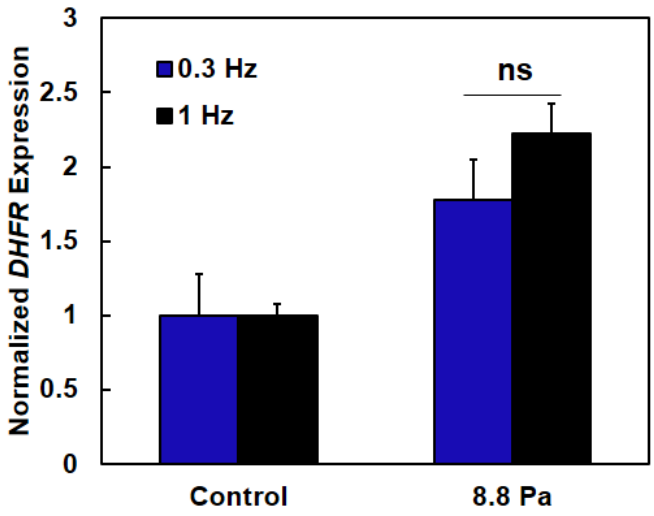

Supplementary Figure 11. Increasing loading frequency does not alter *DHFR* transcription. A 4-mm RGD-bead was bound to the cell surface. A sinusoidal wave cyclic stress was applied at 8.8-Pa at either at 0.3 or 1.0 Hz. The cells in the dish but with no bound beads were used as Control. Mean ± s.e.m.; at 0.3 Hz, n=33 (no stress Control); n=30 (8.8-Pa stress); at 1 Hz, n=34 (no stress Control); n=38 (8.8-Pa stress); 3 separate experiments; ns=not statistically significant.

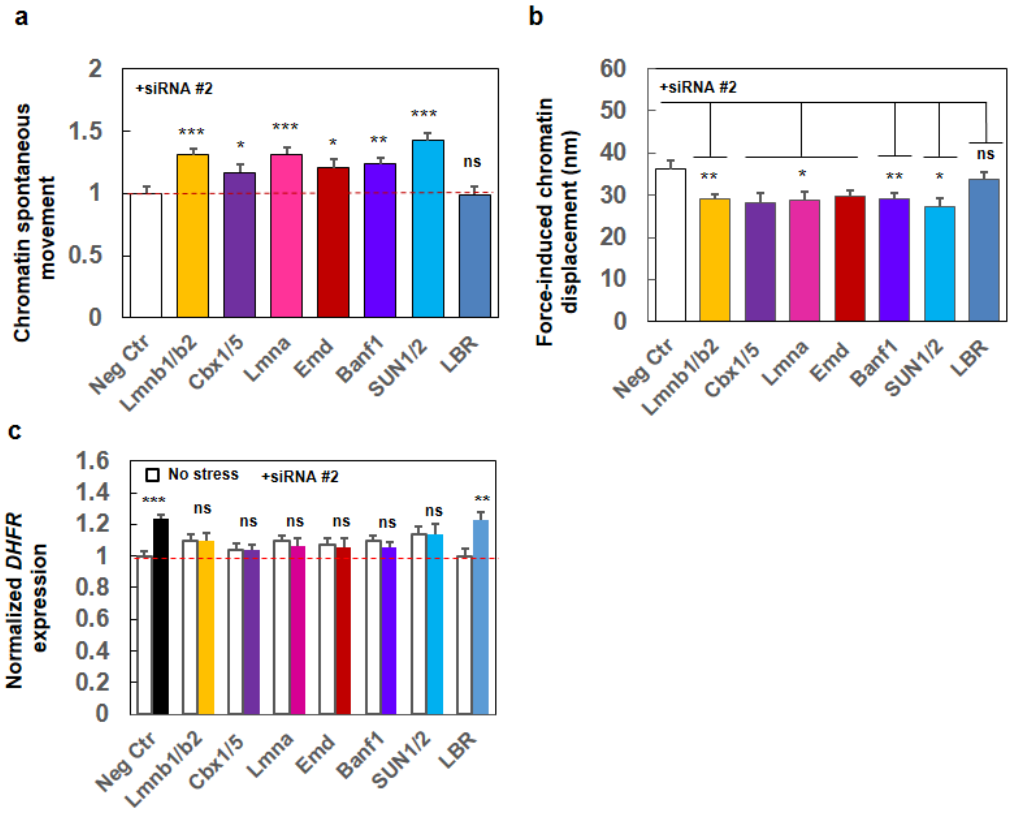

Supplementary Figure 12. Intranuclear proteins tether chromatin to nuclear lamina. All data in this figure are from treatments with #2 siRNAs. (**a**) Summarized data of quantification of the normalized mean (frame-to-frame; 300 ms per frame) chromatin spontaneous movements without externally applied forces. All conditions were normalized to Neg Ctr. **Neg Ctr**: those that were treated with scrambled siRNA. The red dashed line is drawn only for visual aid purpose. Mean ± s.e.m.; n=51 (Neg Ctr), 59 (*Lmnb1/2, both were silenced*), 43 (*cbx1/5, both were silenced*), 60 (*Lmna*), 49 (*Emd*), 53 (*Banf1*), 36 (*Sun1/2, both Sun1 and Sun2 were silenced*), 39 (*LBR*) cells, respectively; 3 independent experiments. * P<0.05; ** P<0.01; *** P<0.001; ns=not statistically significant. Red dashed line is for visual aid only. **(b)** HP1 and BAF proteins, in addition to lamin A, lamin B, Emerin, and SUN1/2, transmit stresses from Lamins to chromatins. *Lmnb1 and 2, Lmna, Emd, Banf1, HP1* (*Cbx1 and 5*), *SUN1/2*, and *LBR* genes were silenced using siRNA and local oscillatory forces are applied to the cell surface using 3D-MTC (8.8 Pa at 0.3 Hz). Force-induced displacements of GFP-LacI labeled chromatin transgenes were measured. **Neg Ctr**: force-induced displacements after scrambled siRNA treatment. Mean ± s.e.m.; n=10, 20, 12, 18, 30, 20, 22, 19 cells for Neg Ctr, *Lmnb1&2, Cbx1&5, Lmna, Emd, and Banf1, SUN1/2, and LBR* respectively; 3 separate experiments; * P<0.05; ** p<0.01; ns=not statistically significant. (**c**) Summarized data for normalized *DHFR* transcription after knocking down individual nuclear proteins. Stress was applied at 17.5 Pa at 0.3 Hz for 2 min to CHO cells bound with RGD-coated magnetic beads. *DHFR* partial transcripts were detected using 5'-probes and FISH. **No stress**: cells in the same dish but no stress was applied. **Neg Ctr**: treated with scrambled siRNA. Mean ± s.e.m.; n=49, 29, 27, 30, 33, 29, 23, and 25 cells for Neg Ctr, Lmnb1/2, Cbx1/5, Lmna, Emd, Banf1, SUN1/2, and LBR silenced conditions under no stress; n=49, 31, 31, 22, 27, 28, 24, and 22, respectively for the corresponding conditions with applied stress. 3 separate experiments. ** P<0.01; *** P<0.001; ns=not statistically significant. Red dashed lines are for visual aid only.

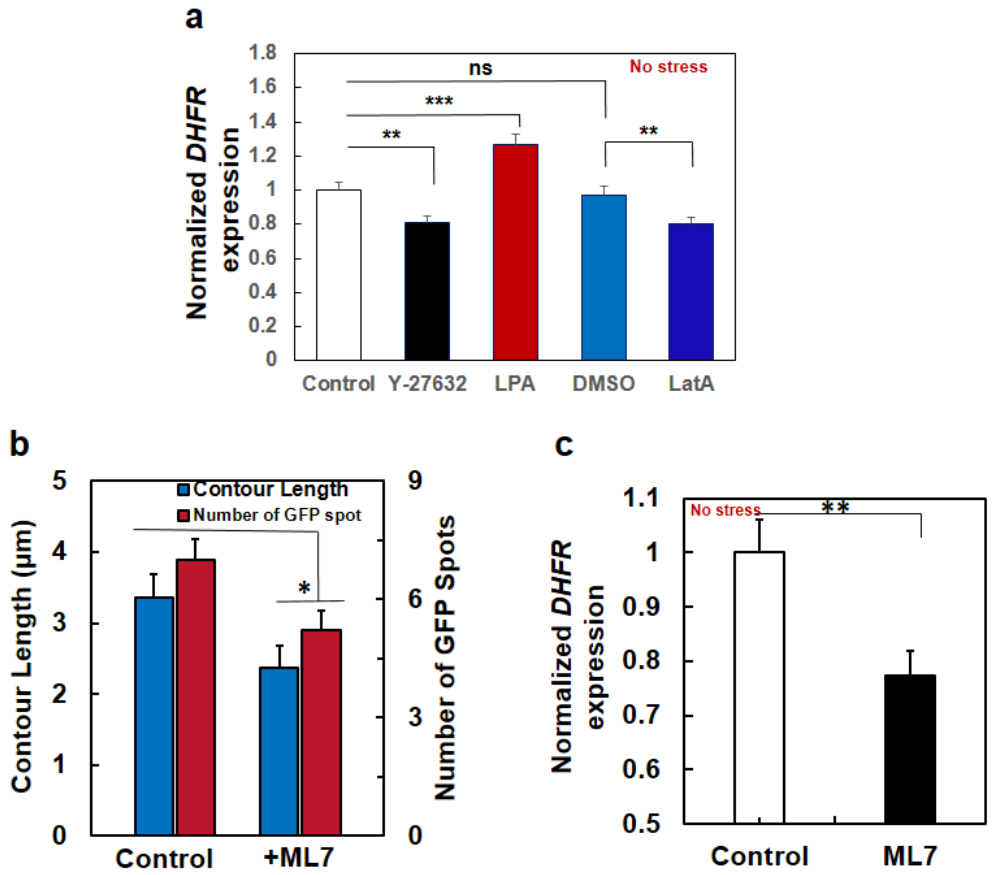

Supplementary Figure 13. Acto-myosin contractility regulates chromatin decondensation and *DHFR* transcription. (a) Modulating endogenous contractility alters *DHFR* transcription in the absence of external forces. **Control**: untreated cells; **Y-27632**: treated with 20 μM Y-27632 for 30 min; **LPA**: treated with 2 μgml^{-1} for 60 min; **DMSO**: treated with 0.1% DMSO for 60 min; **LatA**: treated with 1 μM Latrunculin A for 30 min. Mean ± s.e.m.; n=49 (Control), 43 (Y-27632), 44 (LPA), 41 (DMSO), 55 (LatA) cells, respectively; 3 independent experiments. ** $P<0.01$; *** $P<0.001$; ns=not significantly different. **(b)** Summarized data for contour length (length of the line connecting GFP spots) and the number of GFP spots (number of active transgenes) without (**Control**) and with **ML7** treatment. ML7 treated cells had shorter contour lengths and hence fewer GFP spots, indicating that the chromatin is more condensed. Mean ± s.e.m.; n=10 cells; 3 separate experiments. * $P<0.05$. **(c)** Inhibition of actomyosin contractility downregulates *DHFR* gene expression. Cy3 FISH intensity was used to measure *DHFR* mRNA expression at transgene insertions. Intensity values of ML7 treated cells were normalized by the FISH intensity in untreated control cells (**Control**). Mean ± s.e.m.; n=55 cells; 3 independent experiments. ** $P<0.01$.

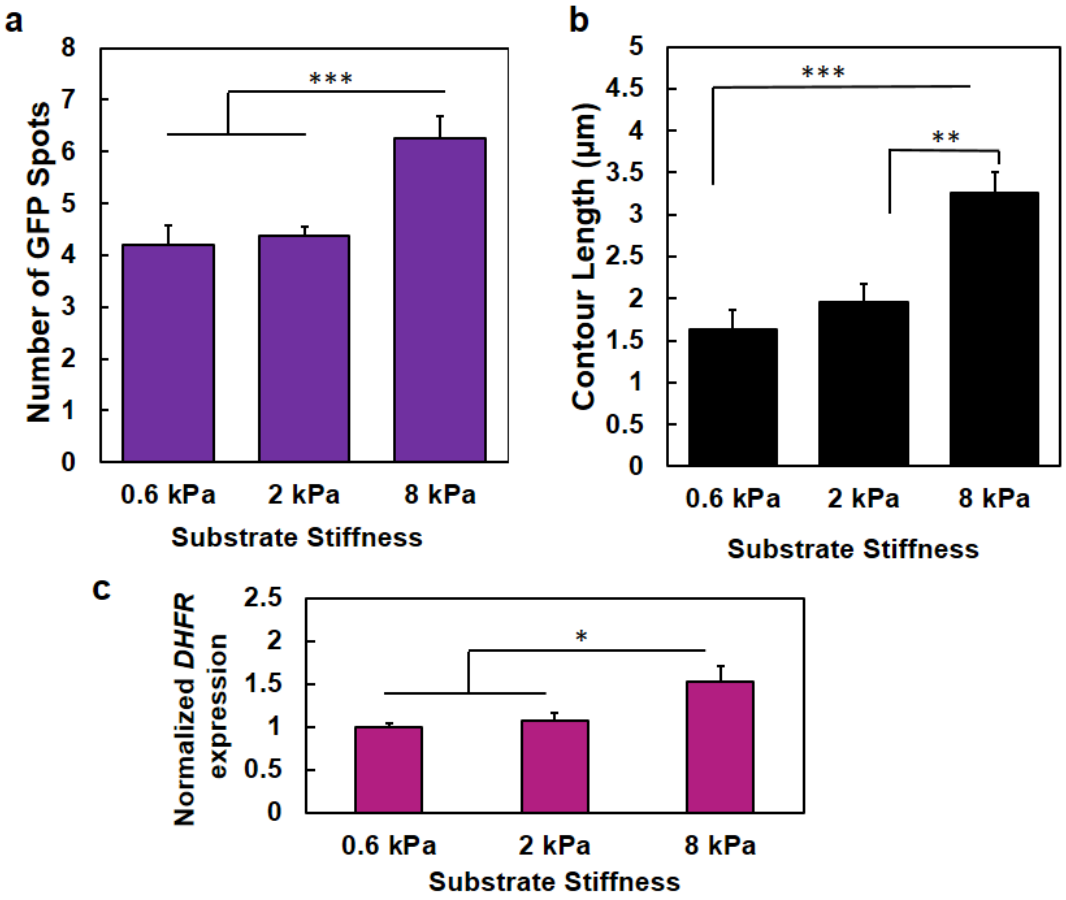

Supplementary Figure 14. Substrate rigidity regulates chromatin organization and *DHFR* transcription. CHO cells were cultured on collagen-1 coated polyacrylamide gels of 0.6, 2, or 8 kPa stiffness **(a)** Number of GFP-LacI spots increases with substrate stiffness. Mean ± s.e.m.; n=10 cells; *** $P<0.001$. **(b)** Contour length increases with substrate stiffness. Mean ± s.e.m.; n=10 cells; ** $P<0.01$; *** $P<0.001$. (**c**) *DHFR* transcription increases with substrate stiffness. Mean ± s.e.m.; n>30 cells in each condition; 4 different experiments; * $P<0.05$.

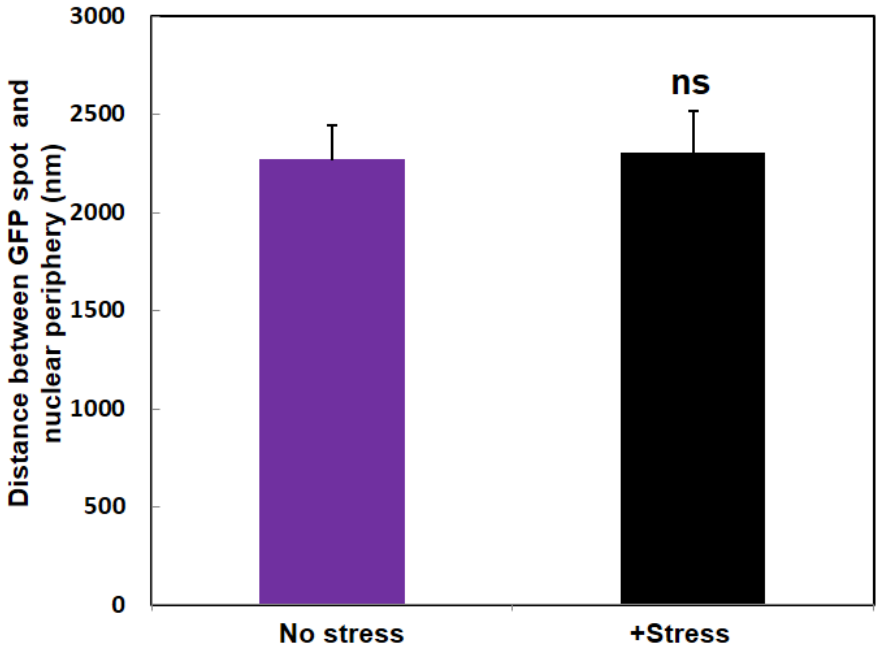

Supplementary Figure 15. Force application does not induce chromatin relocation. CHO cells were cultured on collagen-1 coated glass overnight. A local surface stress (17.5 Pa at 0.3 Hz) was applied via integrins to deform chromatins. The distance between the nuclear periphery and chromatin GFP spots was quantified. **No stress**: the cells with beads before stress was applied. **+Stress**: the same cells after stress was applied for 1 hr. Mean $\pm$ s.e.m.; n=13 cells; 3 separate experiments; ns=not statistically significant; p=0.84.

Supplementary Figure 16. Upregulation of *egr-1* transcription by stress. RGD-coated magnetic beads were attached to the CHO cells for 30 min. **No stress**: cells bound with RGD-beads but no stress was applied. **Stress**: 17.5 Pa stress was applied via magnetic beads at 0.3 Hz for 60 min. mRNAs were collected and assayed for *egr-1* expression using quantitative polymerase chain reaction (PCR). All were normalized by GAPDH. Mean $\pm$ s.e.m., n=3 separate samples; *** $P<0.001$.

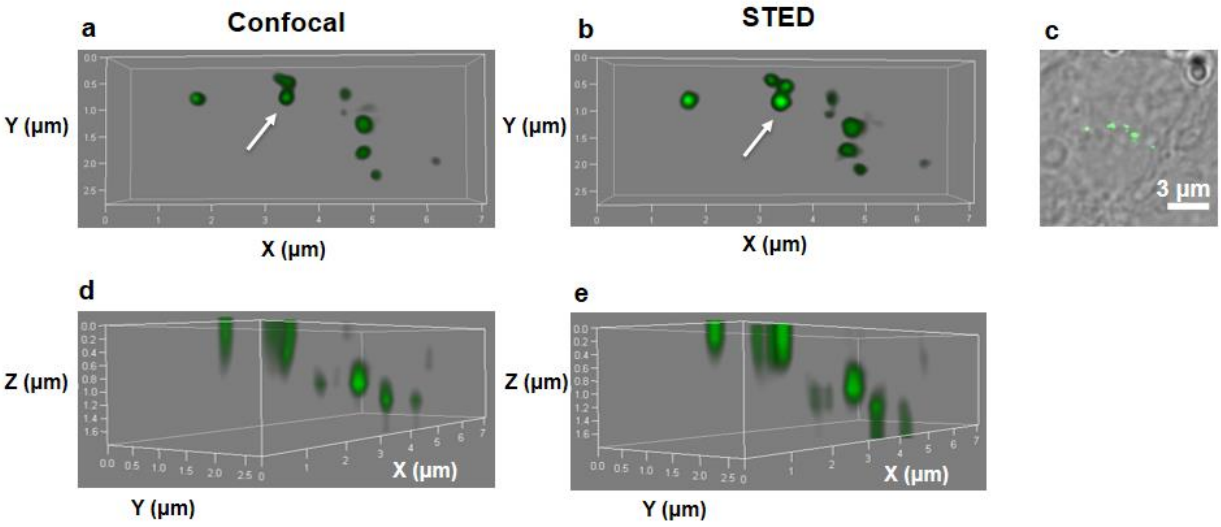

Supplementary Figure 17. Visualization of GFP spots localization in a CHO cells using 3D confocal microscopy and STED nanoscopy. A CHO cell was plated on 100 µg ml^{-1} collagen-1 coated dish overnight. (**a, d**) Images are obtained with confocal microscopy to visualize the GFP spots in a single chromatin in a cell. (**b, e**) Images are obtained with STED nanoscopy for the same GFP spots in the chromatin. (**d**) and (**e**) are oblique views of the GFP spots showing their distribution along the z-axis. (**c**) A brightfield image overlaying with a fluorescent image of GFP-tagged chromatin domains are shown inside the nucleus of a living CHO cell. It appears that there are only 5 to 6 GFP spots with 2D epifluorescence (see **c**) or 7 to 8 GFP spots with confocal microscopy (see **a**). However, with STED (see **b**), one can count a total of 10 GFP spots. **White arrows**: the GFP aggregate that appear to be 1 or 2 GFP spots in confocal in (**a**) but are in fact 3 different GFP spots in STED in (**b**). Two very dim GFP spots in (**a**) and (**b**) are likely due the densely compacted segments of the chromatin such that little GFP-LacI was able to access the LacO spots.

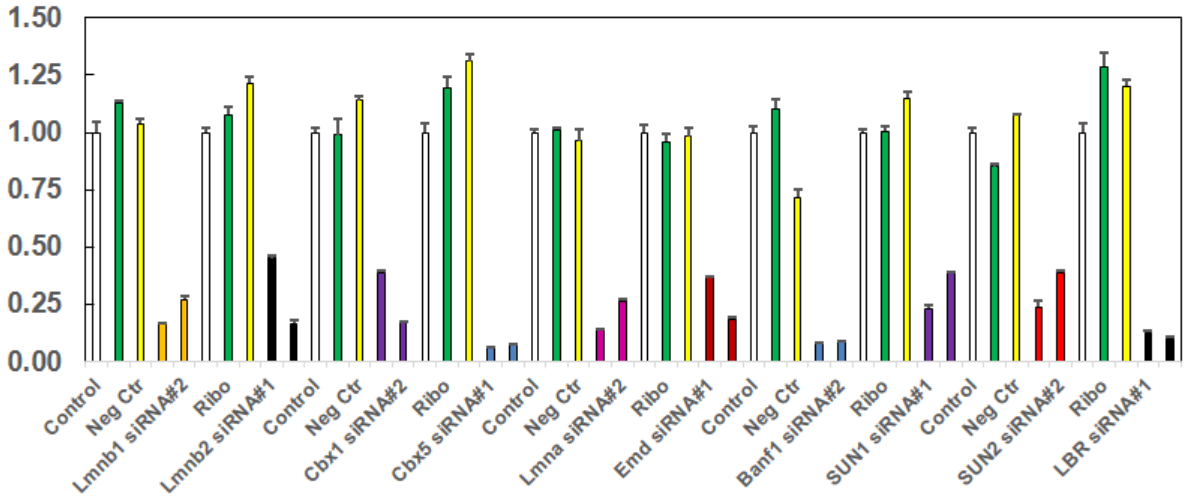

Supplementary Figure 18. Silencing efficiency of various genes in CHO cells. All values are normalized by GAPDH. Control=untreated cells; Ribo= RiboCellin transfection reagent only; Neg Ctr=scrambled siRNA. Two different siRNAs (#1, #2) were used to exclude potential off-target effects. Mean $\pm$ s.e.m; n=3 samples for each condition; all silenced genes were significantly lower than Control or Neg Ctr (all $P<0.001$).

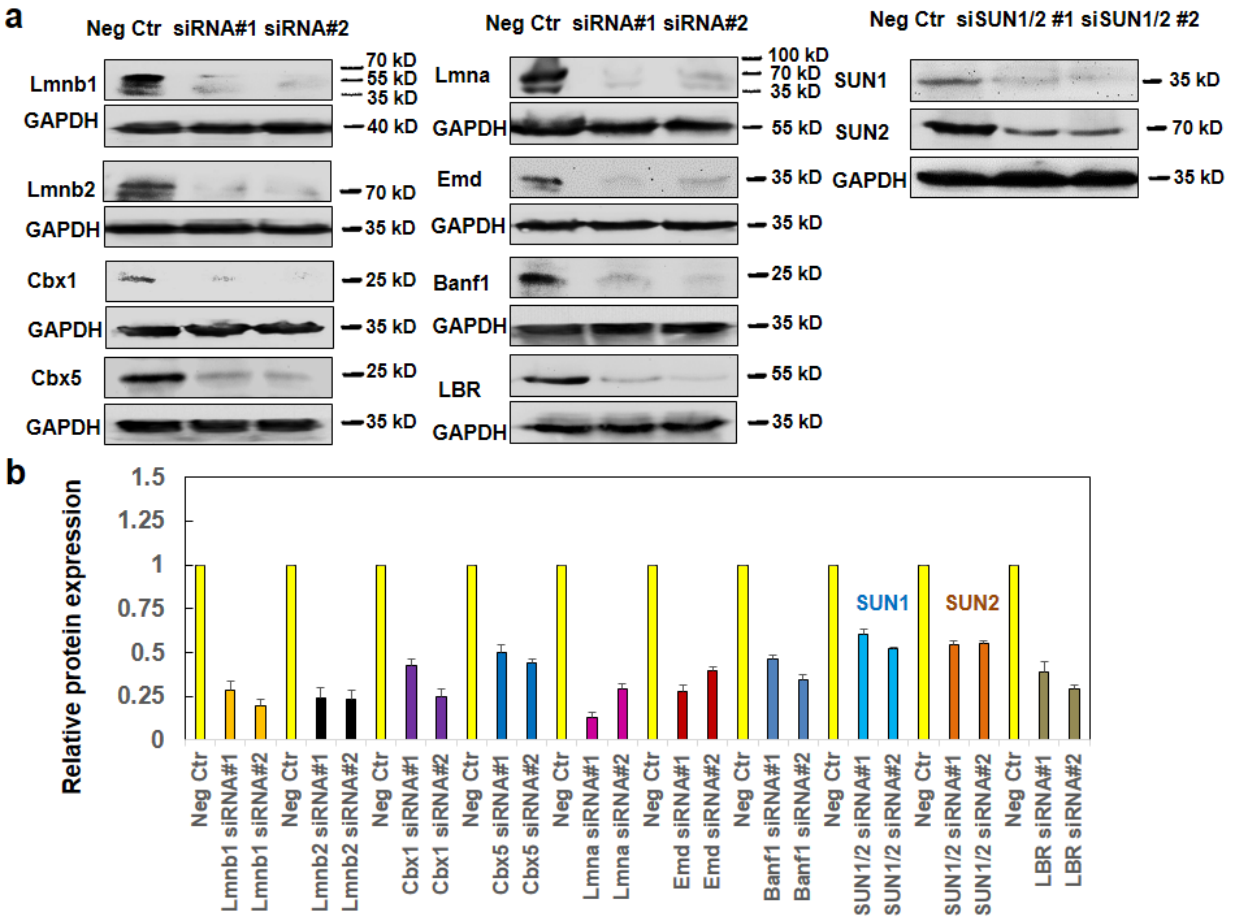

Supplementary Figure 19. Silencing efficiency of various proteins in CHO cells. (**a**) Representative images of Western blotting of various proteins expression after siRNAs knockdown. **Neg Ctr**: treated with scrambled siRNA. Two different siRNAs (#1, #2) were used to exclude potential off-target effects. (**b, c**). Quantification of silencing efficiency on the protein levels. All values are normalized by GAPDH. Mean ± s.e.m; n=3 samples for each condition; all silenced proteins expressions were significantly lower than **Neg Ctr** (all $P<0.01$).